Pergamon

*Computers Math. Applic.* Vol. 27, No. 11, pp. 105–119, 1994

0898-1221/94 $7.00 + 0.00

**0898-1221(94)E0074-T**

# A High Order Difference Method for the Steady State Navier-Stokes Equations

J. Y. Choo and D. H. Schultz
Department of Mathematical Sciences, University of Wisconsin-Milwaukee
Milwaukee, WI 53201, U.S.A.

*(Received and accepted April 1993)*

**Abstract**—A stable high order difference method is developed for solving the heated cavity and the driven cavity problems governed by the steady state Navier-Stokes equations. The numerical results compared favorably with other methods. Coordinate transformations were also used to reflect the boundary layer phenonmena without requiring many mesh points. The methods used in this paper are accurate, stable, and applicable to other flow problems governed by the Navier-Stokes equations.

**Keywords**—Stable, Finite difference method, Navier-Stokes equations, Boundary layer.

## 1. INTRODUCTION

In the present study, we develop a fourth-order numerical method for solving the steady state Navier-Stokes equations governing the flow of an incompressible fluid. The method is an extension of the method developed in [1] and is tested on the heated cavity problem and the driven cavity problem. A coordinate transformation is also tested. For the heated cavity problem, de Vahl Davis and Jones [2] published a paper which summarizes results from 36 sources. Shay and Schultz [3] presented a second-order method and a fourth-order method using extrapolation which compared favorably with the results of de Vahl Davis and Jones. Saitoh and Hirose [4] used a conventional five point fourth-order approximation to obtain a fourth-order method. The disadvantage here is that problems arise near the boundary. They also used a scaled grid spacing with a new transformation function. Dennis and Hudson [5] developed a compact nine-point scheme which is fourth-order accurate. This method is a two-dimensional version of the methods of exponential type. Choo and Schultz [1] presented a fourth-order method which converged for both large $R$ and small Pr. The method is fourth-order without using extrapolation or the upwinding technique. The method is extended here with a coordinate transformation to see if the results can be obtained with a larger mesh size.

In 1968, Greenspan [6,7] and Greenspan and Schultz [8] used the upwind method for solving the driven cavity problem. Since the upwind difference approximation leads to a diagonally dominant system of equations, it proved to be unconditionally stable for any large Reynolds number. In fact, results were obtained [6,7,8] up to a Reynolds number of 100,000.

Many methods have been used to obtain accurate solution for large Reynolds numbers. In 1976, de Vahl Davis and Mallinson [9] used a second order method to obtain the solution for Reynolds numbers up to 5000. A finite element method based on the stream function formulation was presented by Olson and Tunan [10]. Bontoux, Forestier and Roux [11] employed the compact differencing method developed by Hirsh [12]. In 1981, Shay [13] developed a second order method and obtained the solution for Reynolds numbers up to 20,000. More recently (1983), Schreiber

and Keller [14] obtained the solution for Reynolds numbers up to 10,000, using an adaptive Newton-like method for nonlinear systems. Their results seem to be the most comprehensive and reliable so far. Still, they had to use over $100 \times 100$ mesh points to obtain reliable solutions.

The numerical results of this paper compared favorably with those of other methods, especially with [14]. Using a coordinate transformation, we obtained accurate solutions for Reynolds numbers up to 10,000. We did not need to use as many mesh points as in [14] for Reynolds numbers up to 4,000, although we needed more mesh points for the Reynolds numbers 10,000. We employed the SOR method for solving the linear system.

We also tried our method on the biharmonic problem and compared the results to those of a second order method by [15].

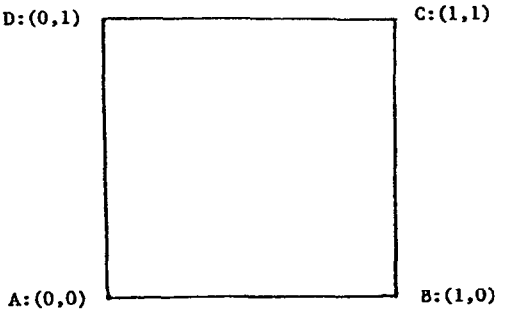


Figure 1.

## 2. THE PROBLEMS

Let $\Omega$ be a square region $(0,1) \times (0,1)$, with vertices $A, B, C, D$, as placed in Figure 1. The heated cavity problem is given by a set of three equations on $\Omega$

$$\Delta\psi = -\omega, \tag{2.1}$$

$$\Delta T + \psi_x T_y - \psi_y T_x = 0, \tag{2.2}$$

$$\Delta\omega + \left(\frac{1}{\mathrm{Pr}}\right)(\psi_x\omega_y - \psi_y\omega_x) + \mathrm{Ra}T_y = 0, \tag{2.3}$$

where $\psi$, $T$ and $\omega$ represent the stream, temperature and vorticity functions. For the case where the surfaces between the hot and cold walls are insulated, the boundary conditions to be satisfied are

$$\psi = 0, \qquad \text{on } ABCDA, \tag{2.4}$$

$$\psi_y = 0, \quad T = 0, \qquad \text{on } AB, \tag{2.5}$$

$$\psi_x = 0, \quad T_x = 0, \qquad \text{on } AD \text{ and } BC, \tag{2.6}$$

$$\psi_y = 0, \quad T = 1, \qquad \text{on } CD. \tag{2.7}$$

The driven cavity problem is given as a set of two equations on $\Omega$

$$\Delta\psi = -\omega, \tag{2.8}$$

$$\Delta\omega + R(\psi_x\omega_y - \psi_y\omega_x) = 0, \tag{2.9}$$

where $\psi$ is the stream function, $\omega$ is the vorticity, and $R$ is the Reynolds number. On $\Omega$ the boundary conditions to be satisfied are

$$\psi = 0, \quad \psi_x = 0, \qquad \text{on } AD, \tag{2.10}$$

$$\psi = 0, \quad \psi_y = 0, \qquad \text{on } AB, \tag{2.11}$$

$$\psi = 0, \quad \psi_x = 0, \qquad \text{on } BC, \tag{2.12}$$

$$\psi = 0, \quad \psi_y = -1, \qquad \text{on } CD. \tag{2.13}$$

# 3. DIFFERENCE METHODS

## 3.1. A Fourth-Order Elliptic Solver

In this section, we shall formulate the difference methods for the given differential equations, which can be seen as special cases of the second-order elliptic equation

$$Lu \equiv u_{xx} + u_{yy} + p(x,y)u_x + q(x,y)u_y + r(x,y)u = s(x,y). \tag{3.1}$$

Letting $p(x,y) = p$, $q(x,y) = q$, $r(x,y) = r$, and $s(x,y) = s$ for simplicity, we may write (3.1) as

$$Lu \equiv u_{xx} + u_{yy} + pu_x + qu_y + ru = s. \tag{3.2}$$

Note that we have $r = 0$, for all given equations, and

| | | | |
|---|---|---|---|
| $p = 0,$ | $q = 0,$ | $s = -\omega,$ | for equation (2.1), |
| $p = -\psi_y,$ | $q = \psi_x,$ | $s = 0,$ | for equation (2.2), |
| $p = -\left(\frac{1}{\mathrm{Pr}}\right)\psi_y,$ | $q = \left(\frac{1}{\mathrm{Pr}}\right)\psi_x,$ | $s = -\mathrm{Ra}T_y,$ | for equation (2.3), |
| $p = 0,$ | $q = 0,$ | $s = -\omega,$ | for equation (2.8), |
| $p = -R\psi_y,$ | $q = R\psi_x,$ | $s = 0,$ | for equation (2.9). |

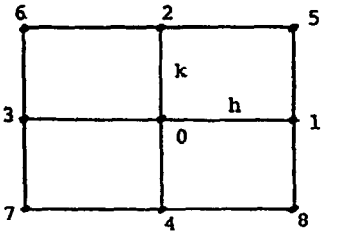


Figure 2.

In addition to the standard central difference formulas for $u_{xx}$, $u_{yy}$, $u_x$ and $u_y$, we shall use the following formulas for the mixed partial derivatives formulated in [16]. Using the notation of Figure 2, we have

$$u_{xy}|_0 = \frac{1}{4hk}(u_7 - u_6 - u_8 + u_5), \tag{3.3}$$

$$u_{xxy}|_0 = \frac{1}{2h^2k}(-u_7 + 2u_4 - u_8 + u_6 - 2u_2 + u_5), \tag{3.4}$$

$$u_{xyy}|_0 = \frac{1}{2hk^2}(-u_7 + 2u_3 - u_6 + u_8 - 2u_1 + u_5), \tag{3.5}$$

$$u_{xxyy}|_0 = \frac{1}{h^2k^2}(u_7 - 2u_4 + u_8 - 2u_3 + 4u_0 - 2u_1 + u_6 - 2u_2 + u_5), \tag{3.6}$$

which are all $O(h^2) + O(k^2)$ accurate (See [16] for the error terms).

Thus, we can employ the fourth-order difference method developed in [16] (for the case $h = k$ see [1]). From [16], we have

$$L^*_{hk}u_0 \equiv \sum_{i=0}^{8} \alpha_i^* u_i = s_0^* + E_0^*[u], \tag{3.7}$$

where

$$s_0^* = s_0 + \frac{h^2}{12}(ps_x + s_{xx})|_0 + \frac{k^2}{12}(qs_y + s_{yy})|_0, \tag{3.8}$$

and

$$
\begin{aligned}
\alpha_0^* &= \frac{-2}{h^2} + \frac{-2}{k^2} + r_0 + 4d - 2e_1 - 2e_2 + rr, \\
\alpha_1^* &= \frac{1}{h^2} + \frac{p_0}{2h} - 2d + e_1 + f_1 + g_1 - 2h_1, \\
\alpha_2^* &= \frac{1}{k^2} + \frac{q_0}{2k} - 2d + e_2 + f_2 + g_2 - 2h_2, \\
\alpha_3^* &= \frac{1}{h^2} - \frac{p_0}{2h} - 2d + e_1 - f_1 - g_1 + 2h_1, \\
\alpha_4^* &= \frac{1}{k^2} - \frac{q_0}{2k} - 2d + e_2 - f_2 - g_2 + 2h_2, \\
\alpha_5^* &= d + h_1 + h_2 + k_1 + k_2, \\
\alpha_6^* &= d - h_1 + h_2 - k_1 - k_2, \\
\alpha_7^* &= d - h_1 - h_2 + k_1 + k_2, \\
\alpha_8^* &= d + h_1 - h_2 - k_1 - k_2,
\end{aligned}
\tag{3.9}
$$

where

$$
\begin{aligned}
d &= \frac{1}{12}\left(\frac{1}{h^2} + \frac{1}{k^2}\right), \\
rr &= \frac{h^2}{12}\left(pr_x + r_{xx}\right)\Big|_0 + \frac{k^2}{12}\left(qr_y + r_{yy}\right)\Big|_0, \\
e_1 &= \frac{1}{12}\left(p^2 + 2p_x + r\right)\Big|_0, \\
e_2 &= \frac{1}{12}\left(q^2 + 2q_y + r\right)\Big|_0, \\
f_1 &= \frac{k^2}{24h}\left(qp_y + p_{yy}\right)\Big|_0, \\
f_2 &= \frac{h^2}{24k}\left(pq_x + q_{xx}\right)\Big|_0, \\
g_1 &= \frac{h}{24}\left(pp_x + pr + p_{xx} + 2r_x\right)\Big|_0, \\
g_2 &= \frac{k}{24}\left(qq_y + qr + q_{yy} + 2r_y\right)\Big|_0, \\
h_1 &= \frac{(h^2 + k^2)}{24hk^2}p_0, \\
h_2 &= \frac{(h^2 + k^2)}{24h^2k}q_0, \\
k_1 &= \frac{h}{48k}\left(pq + 2q_x\right)\Big|_0, \\
k_2 &= \frac{k}{48h}\left(pq + 2p_y\right)\Big|_0.
\end{aligned}
$$

Note that $\alpha_0^*$ is large when $p$ or $q$ is large. Note also that $E_0^*[u]$ is $O(h^m k^n)$ with $m + n = 4$. As mentioned in [1,16], the operator $L_{hk}^*$ is a sixth-order Laplace equation solver if $h = k$ and a fourth-order Poisson equation solver.

Note that for the heated cavity equation (2.2), we have $p = -\psi_y$, $q = \psi_x$, $p_x = -\psi_{xy}$, $p_y = -\psi_{yy}$, $q_x = \psi_{xx}$ and $q_y = \psi_{xy}$. We also have $p_{xx} = -\psi_{xxy}$, $p_{yy} = -\pi_{yyy}$, $q_{xx} = \psi_{xxx}$ and $q_{yy} = \psi_{xyy}$. These values can be approximated with second-order accuracy, using central difference formulas and (3.3)–(3.6), except for $p_{yy}$ and $q_{xx}$. So we need to approximate $p_{yy} = -\psi_{yyy}$ and $q_{xx} = \psi_{xxx}$ with second-order accuracy within the frame of the compact 9-point

stencil, given by Figure 2. This can be done by writing, using equation (2.1)

$$\begin{aligned} \psi_{yyy} &= -(\psi_{xxy} + \omega_y), \\ \psi_{xxx} &= -(\psi_{xyy} + \omega_x). \end{aligned}$$

For a fully fourth-order difference scheme, we need to approximate $p = -\psi_y$ and $q = \psi_x$ with $O(h^4)$ accuracy, which is done as follows:

$$\begin{aligned} \psi_y &= \frac{(-\psi_4 + \psi_2)}{(2k)} - \frac{k^2 \psi_{yyy}}{6} + O(k^4) \\ &= \frac{(-\psi_4 + \psi_2)}{(2k)} + k^2 \frac{(\psi_{xxy} + \omega_y)}{6} + O(k^4). \end{aligned}$$

In a similar way, we obtain

$$\psi_x = \frac{(-\psi_3 + \psi_1)}{(2h)} + h^2 \frac{(\psi_{xyy} + \omega_x)}{6} + O(h^4).$$

We then approximate $\psi_{xxy}$, $\psi_{xyy}$, $\omega_x$ and $\omega_y$ with second-order accuracy using (3.4), (3.5) and central difference formulas.

For the heated cavity equation (2.3), we have $s = -\mathrm{Ra}T_y$. To approximate $s_0^*$, given by (3.8), with fourth-order accuracy, we approximate $s_x = -\mathrm{Ra}T_{xy}$, $s_y = -\mathrm{Ra}T_{yy}$, $s_{xx} = -\mathrm{Ra}T_{xxy}$ and $s_{yy} = -\mathrm{Ra}T_{yyy}$ with second-order accuracy. So we write $T_{yyy}$, using equation (2.2), as

$$T_{yyy} = -(T_{xxy} + \psi_{xy}T_y + \psi_x T_{yy} - \psi_{yy}T_x - \psi_y T_{xy}),$$

which can be approximated with second-order accuracy. We then approximate $s = -\mathrm{Ra}T_y$ by writing

$$s = -\mathrm{Ra}T_y = -\mathrm{Ra}\frac{(-T_4 + T_2)}{(2k)} + \frac{\mathrm{Ra}k^2 T_{yyy}}{6} + O(k^4),$$

where $T_{yyy}$ is given above.

We see that for the driven cavity equations similar results follow directly from those of the heated cavity equations.

### 3.2. The Coordinate Transformation

As a special method of mesh refinement, the coordinate transformation has been tested in papers that studied the driven cavity problem [17,18,19]. Such transformations produce the effect of mesh refinement by concentrating more mesh points in the boundary layer region. Suppose we transform the coordinate system $(x, y)$ to a new coordinate system $(\xi, \eta)$ by the mapping

$$x = g(\xi), \qquad y = h(\eta). \tag{3.10}$$

Then, the original differential equation (3.1) is transformed to a new equation

$$\bar{L}u \equiv a(\xi)u_{\xi\xi} + b(\eta)u_{\eta\eta} + \bar{p}(\xi,\eta)u_\xi + \bar{q}(\xi,\eta)u_\eta + r(\xi,\eta)u = s(\xi,\eta), \tag{3.11}$$

where

$$a(\xi) = \frac{1}{x_\xi^2}, \quad b(\eta) = \frac{1}{y_\eta^2}, \quad \bar{p}(\xi,\eta) = -\frac{x_{\xi\xi}}{x_\xi^3} + \frac{p(\xi,\eta)}{x_\xi}, \quad \text{and} \quad \bar{q}(\xi,\eta) = -\frac{y_{\eta\eta}}{y_\eta^3} + \frac{q(\xi,\eta)}{y_\eta}.$$

We write (3.11) in the simple form

$$\bar{L}u \equiv au_{\xi\xi} + bu_{\eta\eta} + \bar{p}u_\xi + \bar{q}u_\eta + ru = s, \tag{3.12}$$

where

$$a = a(\xi), \quad b = b(\eta), \quad \bar{p} = \bar{p}(\xi,\eta), \quad \bar{q} = \bar{q}(\xi,\eta), \quad r = r(\xi,\eta), \quad \text{and} \quad s = s(\xi,\eta).$$

Note that after the transformation, we have $r = 0$ for all equations and

$$\bar{p} = \frac{-x_{\xi\xi}}{x_\xi^3}, \qquad \bar{q} = \frac{-y_{\eta\eta}}{y_\eta^3}, \qquad s = -\omega, \qquad \text{for equation (2.1)},$$

$$\bar{p} = \frac{-x_{\xi\xi}}{x_\xi^3} - \frac{\psi_\eta}{(x_\xi y_\eta)}, \qquad \bar{q} = \frac{-y_{\eta\eta}}{y_\eta^3} + \frac{\psi_\xi}{(x_\xi y_\eta)}, \qquad s = 0, \qquad \text{for equation (2.2)},$$

$$\bar{p} = \frac{-x_{\xi\xi}}{x_\xi^3} - \frac{(1/\mathrm{Pr})\psi_\eta}{(x_\xi y_\eta)}, \qquad \bar{q} = \frac{-y_{\eta\eta}}{y_\eta^3} + \frac{(1/\mathrm{Pr})\psi_\xi}{(x_\xi y_\eta)}, \qquad s = \frac{-\mathrm{Ra}T_\eta}{y_\eta} \qquad \text{for equation (2.3)},$$

$$\bar{p} = \frac{-x_{\xi\xi}}{x_\xi^3}, \qquad \bar{q} = \frac{-y_{\eta\eta}}{y_\eta^3}, \qquad s = -\omega. \qquad \text{for equation (2.8)},$$

$$\bar{p} = \frac{-x_{\xi\xi}}{x_\xi^3} - \frac{R\psi_\eta}{(x_\xi y_\eta)}, \qquad \bar{q} = \frac{-y_{\eta\eta}}{y_\eta^3} + \frac{R\psi_\xi}{(x_\xi y_\eta)}, \qquad s = 0, \qquad \text{for equation (2.9)}.$$

Then, the fourth-order difference operator $\bar{L}^*_{hk}$ for (3.12) is [16]

$$\bar{L}^*_{hk} u_0 \equiv \sum_{i=0}^{8} \bar{\alpha}^*_i u_i = s^*_0 + \bar{E}^*_0[u], \tag{3.13}$$

where

$$s^*_0 = s_0 + \frac{h^2}{12}\left[\frac{(p - 2a_\xi)\, s_\xi}{a + s_{\xi\xi}}\right]\Big|_0 + \frac{k^2}{12}\left[\frac{(q - 2b_\eta)\, s_\eta}{b + s_{\eta\eta}}\right]\Big|_0, \tag{3.14}$$

and

$$\begin{aligned}
\bar{\alpha}^*_0 &= \frac{-2a_0}{h^2} + \frac{-2b_0}{k^2} + r_0 + 4d - 2e_1 - 2e_2 + rr,\\
\bar{\alpha}^*_1 &= \frac{a_0}{h^2} + \frac{\bar{p}_0}{2h} - 2d + e_1 + f_1 + g_1 - 2h_1,\\
\bar{\alpha}^*_2 &= \frac{b_0}{k^2} + \frac{\bar{q}_0}{2k} - 2d + e_2 + f_2 + g_2 - 2h_2,\\
\bar{\alpha}^*_3 &= \frac{a_0}{h^2} - \frac{\bar{p}_0}{2h} - 2d + e_1 - f_1 - g_1 + 2h_1,\\
\bar{\alpha}^*_4 &= \frac{b_0}{k^2} - \frac{\bar{q}_0}{2k} - 2d + e_2 - f_2 - g_2 + 2h_2,\\
\bar{\alpha}^*_5 &= d + h_1 + h_2 + k_1 + k_2,\\
\bar{\alpha}^*_6 &= d - h_1 + h_2 - k_1 - k_2,\\
\bar{\alpha}^*_7 &= d - h_1 - h_2 + k_1 + k_2,\\
\bar{\alpha}^*_6 &= d + h_1 - h_2 - k_1 - k_2,
\end{aligned} \tag{3.15}$$

where

$$\begin{aligned}
d &= \frac{1}{12}\left(\frac{a}{h^2} + \frac{b}{k^2}\right)\Big|_0,\\
rr &= \frac{h^2}{12}\left[r_{\xi\xi} - \frac{1}{a}\Big((2a_\xi - \bar{p})\, r_\xi\Big)\right]\Big|_0 + \frac{k^2}{12}\left[r_{\eta\eta} - \frac{1}{b}\Big((2b_\eta - \bar{q})\, r_\eta\Big)\right]\Big|_0,\\
e_1 &= \frac{1}{12}\left[a_{\xi\xi} + 2\bar{p}_\xi + r - \frac{1}{a}\Big((2a_\xi - \bar{p})\,(a_\xi + \bar{p})\Big)\right]\Big|_0,\\
e_2 &= \frac{1}{12}\left[b_{\eta\eta} + 2\bar{q}_\eta + r - \frac{1}{b}\Big((2b_\eta - \bar{q})\,(b_\eta + \bar{q})\Big)\right]\Big|_0,
\end{aligned}$$

$$f_1 = \frac{k^2}{24h}\left[\bar{p}_{\eta\eta} - \frac{1}{b}\Big((2b_\eta - \bar{q})\bar{p}_\eta\Big)\right]\Big|_0,$$

$$f_2 = \frac{h^2}{24k}\left[\bar{q}_{\xi\xi} - \frac{1}{a}\Big((2a_\xi - \bar{p})\bar{q}_\xi\Big)\right]\Big|_0,$$

$$g_1 = \frac{h}{24}\left[\bar{p}_{\xi\xi} + 2r_\xi - \frac{1}{a}\Big((2a_\xi - \bar{p})(\bar{p}_\xi + r)\Big)\right]\Big|_0,$$

$$g_2 = \frac{k}{24}\left[\bar{q}_{\eta\eta} + 2r_\eta - \frac{1}{b}\Big((2b_\eta - \bar{q})(\bar{q}_\eta + r)\Big)\right]\Big|_0,$$

$$h_1 = \frac{h}{24k^2}\left[-\frac{1}{a}\Big((2a_\xi - \bar{p})b\Big)\right]\Big|_0 + \frac{\bar{p}_0}{24h},$$

$$h_2 = \frac{k}{24h^2}\left[-\frac{1}{b}\Big((2b_\eta - \bar{q})a\Big)\right]\Big|_0 + \frac{\bar{q}_0}{24k},$$

$$k_1 = \frac{h}{48k}\left[2\bar{q}_\xi - \frac{1}{a}\Big((2a_\xi - \bar{p})\bar{q}\Big)\right]\Big|_0,$$

$$k_2 = \frac{k}{48h}\left[2\bar{p}_\eta - \frac{1}{b}\Big((2b_\eta - \bar{q})\bar{p}\Big)\right]\Big|_0.$$

Note that $\bar{E}_0^*[u]$ is $O(h^m k^n)$ with $m + n = 4$.

Note that, for each transformed equation, we can approximate $\bar{p}_\xi$, $\bar{p}_\eta$, $\bar{p}_{\xi\xi}$, $\bar{p}_{\eta\eta}$, $\bar{q}_\xi$, $\bar{q}_\eta$, $\bar{q}_{\xi\xi}$ and $\bar{q}_{\eta\eta}$ as before by writing

$$\psi_{\eta\eta\eta} = -\frac{1}{b}\Big[a\psi_{\xi\xi\eta} + \bar{p}\psi_{\xi\eta} + (\bar{q} + b_\eta)\psi_{\eta\eta} + \bar{q}_\eta\psi_\eta + \omega_\eta\Big],$$

$$\psi_{\xi\xi\xi} = -\frac{1}{a}\Big[b\psi_{\xi\eta\eta} + \bar{q}\psi_{\xi\eta} + (\bar{p} + a_\xi)\psi_{\xi\xi} + \bar{p}_\xi\psi_\xi + \omega_\xi\Big],$$

and

$$T_{\eta\eta\eta} = -\frac{1}{b}\Big[aT_{\xi\xi\eta} + \bar{p}T_{\xi\eta} + \bar{p}_\eta T_\eta + (\bar{q} + b_\eta)T_{\eta\eta} + \bar{q}_\eta T_\eta\Big].$$

## 4. ON AND NEAR THE BOUNDARY

In the previous section, we formulated the difference methods for the given equations. In this section, we shall present the difference equations for each problem on and near the boundary.

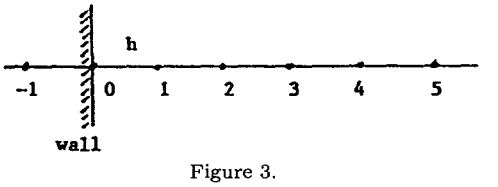


Figure 3.

### 4.1. The Heated Cavity Problem

As we discussed in [1], using the notation in Figure 3, we evaluate $\omega$ on the boundary $AD$ and $BC$ by

$$\omega_0 = -\psi_{xx}\big|_0 = \frac{-1}{60h^2}\Big(225\psi_0 - 770\psi_1 + 1070\psi_2 - 780\psi_3 + 305\psi_4 - 50\psi_5\Big) + O\left(h^4\right). \tag{4.1}$$

The same formula with $h$ replaced by $k$ is used for $\omega = -\psi_{yy}$ on $AB$ and $CD$. In the case of the coordinate transformation, (4.1) becomes

$$\omega_0 = -\left.\frac{\psi_{\xi\xi}}{x_\xi^2}\right|_0 = \frac{-1}{60h^2}\frac{1}{x_\xi^2|_0}\Big(225\,\psi_0 - 770\,\psi_1 + 1070\,\psi_2 - 780\,\psi_3 + 305\,\psi_4 - v50\,\psi_5\Big) + O\left(h^4\right).$$

For the case $T_x = 0$ on the side boundaries, we use as in [1]

$$T_{-1} = \frac{1}{2}\Big( - 3T_0 + 6T_1 - T_2\Big) + O\left(h^4\right). \tag{4.2}$$

The coordinate transformation does not change the form of this difference equation.

For the stream values on the inner boundary, i.e., on the set of all points that lie a distance $h$ from the boundary [6], we use as in [1]

$$\psi_1 = \frac{\psi_2}{2} - \frac{\psi_3}{9} + O\left(h^4\right) \tag{4.3}$$

or

$$\psi_1 = \frac{3\psi_2}{4} - \frac{\psi_3}{3} + \frac{\psi_4}{16} + O\left(h^5\right). \tag{4.4}$$

The coordinate transformation does not change the form of these difference equations.

### 4.2. The Driven Cavity Problem

As we have done for the heated cavity problem, we derive stream values on the inner boundary from the difference formulas:

$$\psi_x\big|_0 = \frac{1}{(\pm 6h)}\Big( - 11\psi_0 + 18\psi_1 - 9\psi_2 + 2\psi_3\Big) + O(h^3) \quad \text{and}$$

$$\psi_y\big|_0 = \left(-11\psi_0 + 18\psi_1 - 9\psi_2 + 2\psi_3\right) + O(k^3)$$

$$\psi_1 = \frac{\psi_2}{2} - \frac{\psi_3}{9}, \qquad \text{near } AD,\ AB,\ BC, \tag{4.5}$$

$$\psi_1 = \frac{\psi_2}{2} - \frac{\psi_3}{9} + \frac{k}{3}, \qquad \text{near } CD. \tag{4.6}$$

Note that the formula (4.6) is different from the others because of the boundary condition (2.13). The coordinate transformation gives

$$\psi_1 = \frac{\psi_2}{2} - \frac{\psi_3}{9} + \frac{k\, y_\eta\big|_0}{3}, \qquad \text{near } CD, \tag{4.7}$$

since $\psi_\eta = -y_\eta$ from $\psi_y = \psi_\eta / y_\eta = -1$ on $CD$.

Since there is no explicit boundary condition for $\omega$, we need to update boundary vorticities. There have been a variety of difference schemes for approximating $\omega$ on the boundary (see [9] or [13]). Bozeman and Dalton [20] noted that some approximations may lead to numerical instability.

Using the boundary conditions (2.10)–(2.13) and the notation in Figure 2, Schreiber and Keller [14] evaluated $\psi$ on the outer boundary as follows.

$$\psi_{-1} = \psi_1 - 2h\,\psi_x\big|_0 = \psi_1, \qquad \text{on } AD, \tag{4.8}$$

$$\psi_{-1} = \psi_1 - 2k\,\psi_y\big|_0 = \psi_1, \qquad \text{on } AB, \tag{4.9}$$

$$\psi_{-1} = \psi_1 + 2h\,\psi_x\big|_0 = \psi_1, \qquad \text{on } BC, \tag{4.10}$$

$$\psi_{-1} = \psi_1 + 2k\,\psi_y\big|_0 = \psi_1 - 2k, \qquad \text{on } CD. \tag{4.11}$$

Using the central difference formulas with the boundary conditions (2.10)–(2.13), we get from (2.8)

$$\omega_0 = -\psi_{xx}\big|_0 = -\frac{2\psi_1}{h^2}, \qquad \text{on } AD, \tag{4.12}$$

$$\omega_0 = -\psi_{yy}\big|_0 = -\frac{2\psi_1}{k^2}, \qquad \text{on } AB, \tag{4.13}$$

$$\omega_0 = -\psi_{xx}\big|_0 = -\frac{2\psi_1}{h^2}, \qquad \text{on } BC, \tag{4.14}$$

$$\omega_0 = -\psi_{yy}\big|_0 = -\frac{(2\psi_1 - 2k)}{k^2}, \qquad \text{on } CD. \tag{4.15}$$

The difference equations (4.12)–(4.15) become after coordinate transformation

$$\omega_0 = -\left[a(\xi)\psi_{\xi\xi} + \bar{p}(\xi,\eta)\psi_\xi\right]\big|_0 = -\frac{2a_0\psi_1}{h^2}, \qquad \text{on } AD, \tag{4.16}$$

$$\omega_0 = -\left[b(\eta)\psi_{\eta\eta} + \bar{q}(\xi,\eta)\psi_\eta\right]\big|_0 = -\frac{2b_0\psi_1}{k^2}, \qquad \text{on } AB, \tag{4.17}$$

$$\omega_0 = -\left[a(\xi)\psi_{\xi\xi} + \bar{p}(\xi,\eta)\psi_\xi\right]\big|_0 = -\frac{2a_0\psi_1}{h^2}, \qquad \text{on } BC, \tag{4.18}$$

$$\omega_0 = -\left[b(\eta)\psi_{\eta\eta} + \bar{q}(\xi,\eta)\psi_\eta\right]\big|_0 = -\frac{2b_0\psi_1}{k^2} - \frac{y_{\eta\eta}y_\eta}{y_\eta^3}\bigg|_0, \qquad \text{on } CD. \tag{4.19}$$

## 5. RESULTS AND CONCLUSIONS

We first tried the method on the biharmonic problem $\Delta(\Delta u) = 0$, such that the exact solution is (a) $u = x^5 - 2x^3y^2 - 3xy^4$ and (b) $u = xe^x \cos y$. For case (a) the relative error given by the present method was $0.19 \times 10^{-16}$ for $h = 1/8$ and for case (b) it was $0.19 \times 10^{-6}$ for $h = 1/10$. A second order method [15] gave $0.26 \times 10^{-2}$ and $0.19 \times 10^{-3}$, respectively. The relative error was measured by the $l^2$ norm.

The heated cavity problem, given by the equations (2.1)–(2.3), was solved via the coordinate transformation

$$x = \frac{1}{2} + \frac{1}{2}\frac{\tanh\left(c(2\xi - 1)\right)}{\tanh(c)}; \qquad y = \frac{1}{2} + \frac{1}{2}\frac{\tanh\left(c(2\eta - 1)\right)}{\tanh(c)}. \tag{5.1}$$

We carried out the computation on the uniform mesh of the domain $(0,1) \times (0,1)$ in the $(\xi,\eta)$ coordinate-plane and obtained the solution on the nonuniform mesh of the domain $(0,1) \times (0,1)$ in the $(x,y)$ coordinate-plane. Note that we can have more points concentrated in the region of the boundary layers by increasing $c$ in the mapping (5.1). The numerical results by the present method via coordinate transformation (5.1) are given in Table 1.

We see that the present results via coordinate transformation show a much better convergence for $\mathrm{Ra} = 10^5$ and $\mathrm{Ra} = 10^6$ in comparison to those without coordinate transformation [1]. That is, for $\mathrm{Ra} = 10^5$ the present results with $n = 80$ are comparable to those with $n = 100$ in [1], and for $\mathrm{Ra} = 10^6$ the present results with $n = 80$ are comparable to those with $n = 120$ in [1].

As for the driven cavity problem, various methods have been used to cope with the boundary layer behavior. For example, de Vahl Davis [9] used variable coefficients in the region near $CD$. Others [14] simply used very small mesh size, as small as $h = k = 1/180$. However, papers [17–19] obtained good results using the coordinate transformation (5.1). The present fourth-order method using the mapping (5.1) was run for a variety of Reynolds numbers, denoted as $R$. Since most papers present their results for $R = 1,000$, we compare these results with ours in Table 2. The results agree fairly well. Note that the coordinate transformation does not require many mesh points, which the method by Mei [19] and the present method clearly indicate. The reason

Table 1. Comparison of the present fourth order results via coordinate transformation as a function of Ra and $n$ (Pr = 0.71).

| | | $n = 20$ | $n = 40$ | $n = 60$ | $n = 80$ |
|---|---|---|---|---|---|
| $\mathrm{Ra} = 10^3$ | $\psi_{\mathrm{mid}}$ | 1.1766 | 1.1746 | 1.1746 | 1.1746 |
| $c = .8$ | $\psi_{\max}$ | 1.1766 | 1.1746 | 1.1746 | 1.1746 |
| | | $n = 20$ | $n = 40$ | $n = 60$ | $n = 80$ |
| $\mathrm{Ra} = 10^4$ | $\psi_{\mathrm{mid}}$ | 5.0775 | 5.0744 | 5.0738 | 5.0736 |
| $c = .7$ | $\psi_{\max}$ | 5.0775 | 5.0744 | 5.0738 | 5.0736 |
| | | $n = 20$ | $n = 40$ | $n = 60$ | $n = 80$ |
| $\mathrm{Ra} = 10^5$ | $\psi_{\mathrm{mid}}$ | 8.966 | 9.1170 | 9.1171 | 9.1163 |
| $c = .8$ | $\psi_{\max}$ | 9.4065 | 9.6091 | 9.6186 | 9.6165 |
| | | $n = 40$ | $n = 60$ | $n = 80$ | $n = 100$ |
| $\mathrm{Ra} = 10^6$ | $\psi_{\mathrm{mid}}$ | 16.1965 | 16.3584 | 16.3839 | 16.3875 |
| $c = .8$ | $\psi_{\max}$ | 16.5794 | 16.7793 | 16.8078 | 16.8071 |

Table 2. Comparison of vortex center data for $R = 1,000$. $n \times m$ denotes the number of mesh points, and $\psi_{vc}$ and $\omega_{vc}$ denote the stream function value and vorticity value at the vortex center.

| Reference | $n \times m$ | $\psi_{vc}$ | $\omega_{vc}$ | Vortex center |
|---|---|---|---|---|
| Rubin [21] | 66×66 | 0.114 | 1.985 | (0.52, 0.56) |
| Shay [13] | 81×81 | 0.1132 | 2.08 | (0.52, 0.58) |
| Ghia [22] | 129×129 | 0.1179 | 2.04 | (0.531, 0.593) |
| Schreiber [14] | 141×141 | 0.1160 | 2.027 | (0.529, 0.564) |
| Mei [19] | 41×41 | 0.1179 | 2.07 | (0.531, 0.593) |
| this paper | 61×81 | 0.1183 | 2.063 | (0.523, 0.568) |

Table 3. Comparison of convergence for $R = 1,000$.

| Reference | $h$ | $\psi_{vc}$ | $\omega_{vc}$ |
|---|---|---|---|
| Schreiber and Keller [14] | 1/100 | 0.11315 | 1.9863 |
| | 1/120 | 0.11492 | 2.0112 |
| | 1/140 | 0.11603 | 2.0268 |
| | extrapolated | 0.11894 | 2.0677 |
| this paper (without transformation) | 1/30 | 0.11415 | 2.0097 |
| | 1/60 | 0.11659 | 2.0678 |
| | 1/80 | 0.11733 | 2.0602 |
| | 1/120 | 0.11826 | 2.0627 |
| this paper (with transformation) | 1/40 | 0.11377 | 2.0204 |
| | 1/60 | 0.11750 | 2.0526 |
| | 1/80 | 0.11854 | 2.0667 |

Table 4. Comparison of results: Stream function and vorticity at the vortex center.

| Reference | $R$ | $n \times m$ | $\psi_{vc}$ | $\omega_{vc}$ |
|---|---|---|---|---|
| Schreiber and Keller [14] | 100 | 121×121 | 0.10330 | 3.18200 |
| | 400 | 141×141 | 0.11297 | 2.28100 |
| | 1,000 | 141×141 | 0.11603 | 2.02600 |
| | 4,000 | 161×161 | 0.11237 | 1.80500 |
| | 10,000 | 181×181 | 0.10284 | 1.62200 |
| this paper (with transformation) | 100 | 41×61 | 0.10348 | 3.16953 |
| | 400 | 41×61 | 0.11373 | 2.27698 |
| | 1,000 | 61×81 | 0.11830 | 2.06271 |
| | 4,000 | 61×81 | 0.11333 | 1.80489 |
| | 10,000 | 61×81 | 0.10157 | 1.62078 |

why the uniform mesh require a very small mesh size is because it cannot adapt to the rapid change of vorticity values in the boundary layer region, mainly near $CD$ (see Figure 1).

We now compare the convergence of the numerical solution by the present method with that of Schreiber and Keller [14]. We present this in Table 3. Note that the numerical results of the present method are reliable already with $h = 1/40$, which is comparable to the results of the method by Schreiber and Keller with $h = 1/120$. Note also that the extrapolated values of the method by Schreiber and Keller are close to our results with $h = 1/80$. We could obtain consistent results for a wide range of $c$. For large Reynolds numbers, however, the results were somewhat sensitive to the choice of $c$. Without the transformation, the method worked well up to about $R = 4,000$. Above $R = 4000$ the results were not as good. Table 4 compares the present results with those of Schreiber and Keller [14] for various $R$.

In the following pages, we show some of the graphic description of the heated cavity flow (Figures 4–6), and of the driven cavity flow (Figures 7–10). In Figures 7–10, we used the same level values for the stream function and vorticities as did Schreiber and Keller [14]. That is, we identified stream lines with 0.11, 0.10, 0.08, 0.06, 0.04, 0.02, 0.01, 0.0, $-0.00001$, $-0.0001$, $-0.001$, $-0.002$ and the vorticities with 5, 3, 1, $-1$, $-3, 5$. The stream lines and vorticity lines fairly well agree with those given by reference [14]. We see that the vorticity lines move toward the walls as $R$ increases.

The present method worked very well for the tested problems, particularly the biharmonic problem and the heated cavity problem. The method is general and can be applied to other partial differential equations.

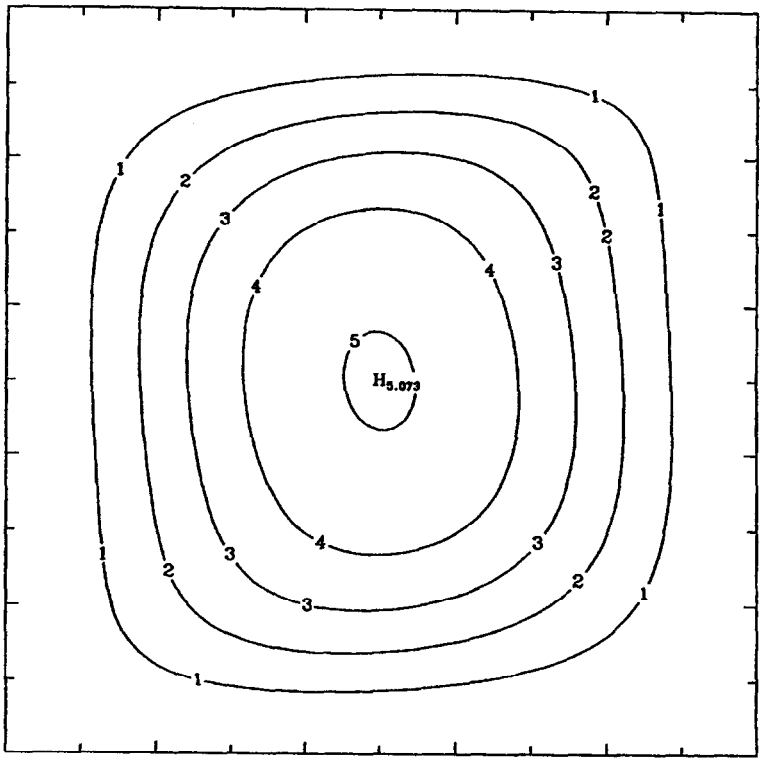


Figure 4. Streamlines for Ra = $10^4$ and Pr = 0.71, 60 × 60 grid.

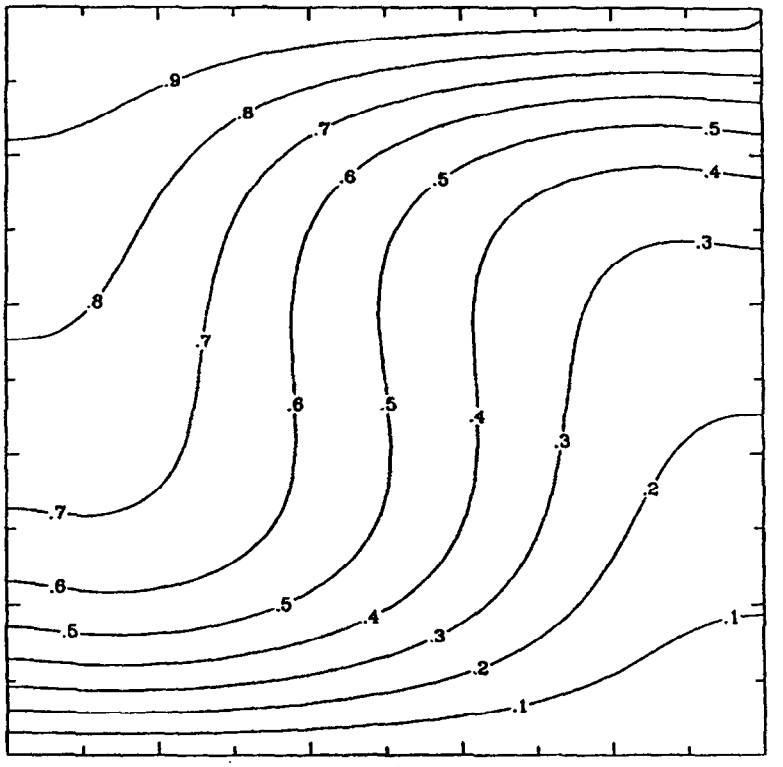


Figure 5. Temperature for Ra = $10^4$ and Pr = 0.71, 60 x 60 grid.

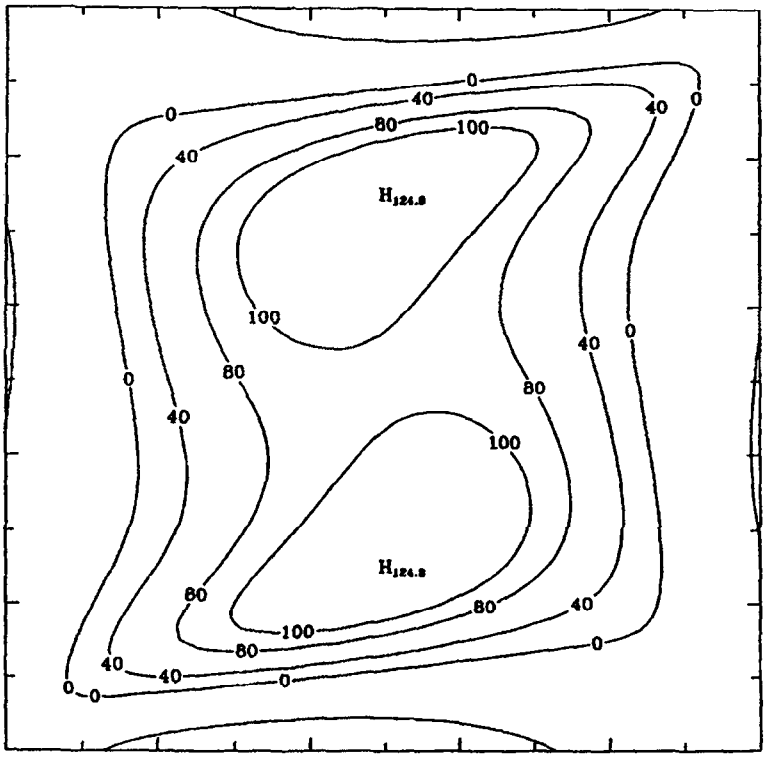


Figure 6. Vorticities for Ra = $10^4$ and Pr = 0.71, 60 x 60 grid.

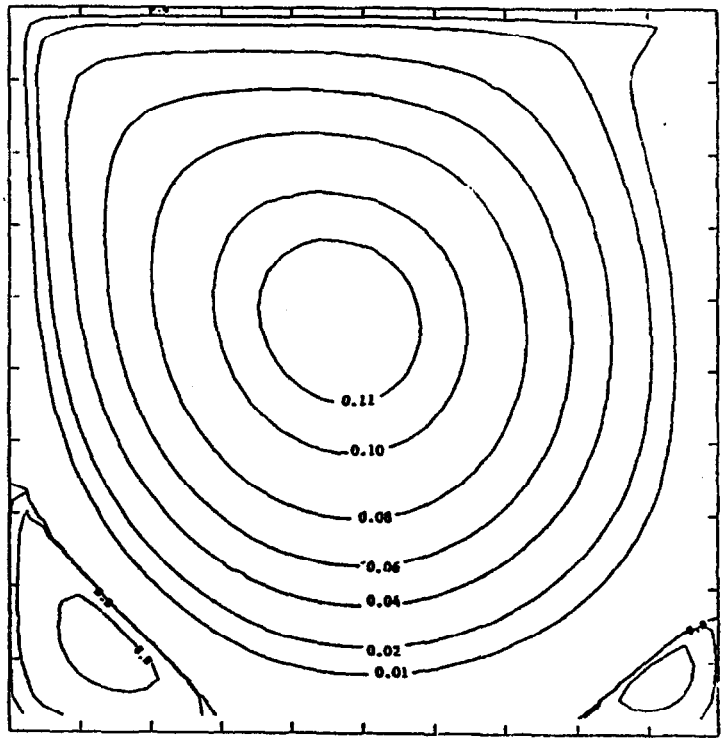


Contour from $-0.20000\text{E} - 02$ to 0.11000; contour interval of irregular; $x$ interval $= 0.10000$; $y$ interval $= 0.10000$.

Figure 7. Stream lines for $R = 1,000$, $40 \times 60$ grid.

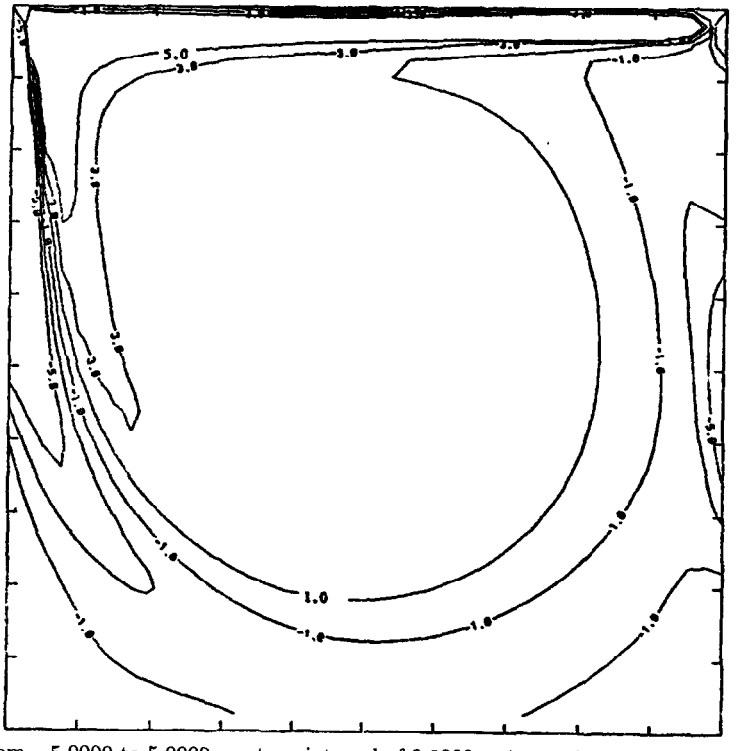


Contour from $-5.0000$ to 5.0000; contour interval of 2.0000; $x$ interval $= 0.10000$; $y$ interval $= 0.10000$.

Figure 8. Vorticity lines for $R = 1,000$, $40 \times 60$ grid.

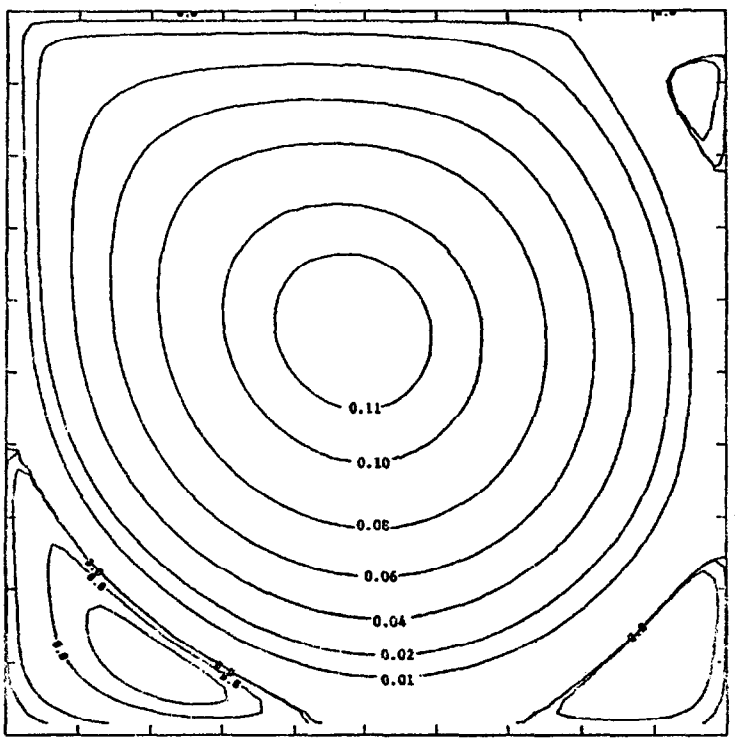


Contour from $-0.20000\text{E}-02$ to 0.11000; contour interval of irregular; $x$ interval = 0.10000; $y$ interval = 0.10000.

Figure 9. Stream lines for $R = 4,000$, $60 \times 80$ grid.

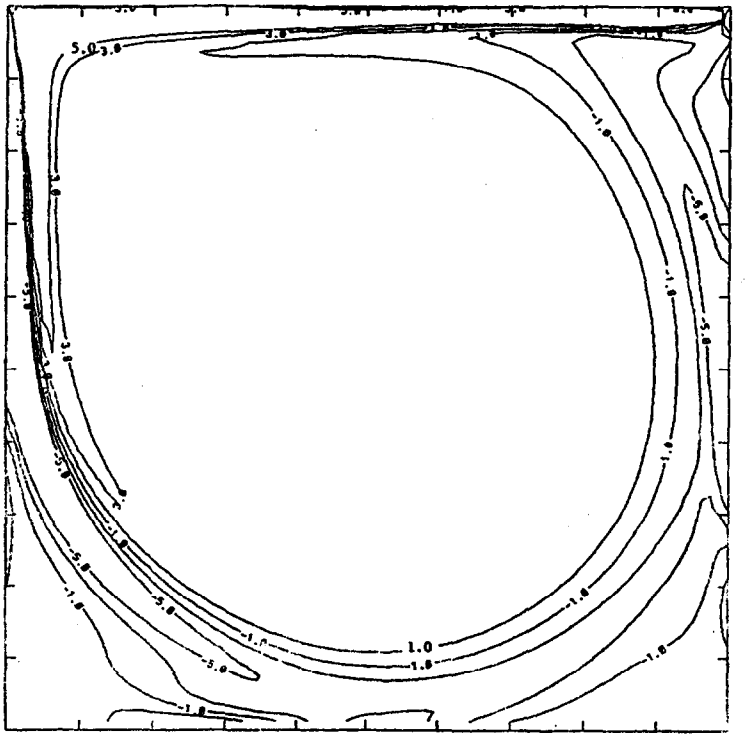


Contour from $-5.0000$ to 5.0000; contour interval of 2.0000; $x$ interval = 0.10000; $y$ interval = 0.10000.

Figure 10. Vorticity lines for $R = 4,000$, $60 \times 80$ grid.

# REFERENCES


1. J.Y. Choo and D.H. Schultz, A stable high order method for the heated cavity problem, *Int. J. for Numerical Methods in Fluids* **15**, 1313–1332 (1992).
2. G. de Vahl Davis and I.P. Jones, Natural convection in a square cavity: A comparison exercise, *Int. J. for Numerical Methods in Fluids* **3**, 227–248 (1983).
3. W.A. Shay and D.H. Schultz, A second-order approximation to natural convection for large Rayleigh numbers and small Prandtl numbers, *Int. J. for Numerical Methods in Fluids* **5**, 427–438 (1985).
4. T. Saitoh and K. Hirose, High-accuracy bench mark solutions to natural convection in a square cavity, *Comput. Mech.* **4**, 417–427 (1989).
5. S.C.R. Dennis and J.D. Hudson, Compact $h^4$ finite-difference approximations to operators of Navier-Stokes type, *Journal of Computational Physics* **85**, 390–416 (1989).
6. D. Greenspan, *Lectures on the Numerical Solution of Linear, Singular and Nonlinear Differential Equations*, Prentice-Hall, Englewood Cliffs, NJ, (1968).
7. D. Greenspan, Numerical studies of prototype cavity flow problems, *Computer Journal* **12** (1969).
8. D. Greenspan and D. Schultz, Simplification and improvement of a numerical method for Navier-Stokes problems, In *Proceeding of the Colloquium on Differential Equations of the Bolyai Janos Mathematical Society*, Hungary, (1975).
9. G. de Vahl Davis and G.D. Mallinson, An evaluation of upwind and central difference approximations by a study of recirculating flow, *Computers & Fluids* **4**, 29–43 (1976).
10. M.D. Olson and S.Y. Tunan, New finite element results for the square cavity, *Computers and Fluids* **7**, 123–135 (1979).
11. P. Bontoux, B. Frestier and B. Roux, Analysis of higher order methods for the numerical simulation of confined flows, In $6^{th}$ *Int. Conf. Numer. Meth. Fluid Dyn.*, Tbilisi U.S.S.R., Springer-Verlag, Berlin, (1978).
12. R.S. Hirsh, Higher order accurate difference solutions of fluid mechanics problems by a compact differencing technique, *J. Comput. Phys.* **85** (19), 90–10 (1975).
13. W.A. Shay, Development of a second order approximation for the Navier-Stokes equations, Ph.D. Thesis, University of Wisconsin-Milwaukee, (1978).
14. R. Schreiber and H.B. Keller, Driven cavity flows by efficient numerical techniques, *J. Comput. Physics.* **49**, 310–333 (1983).
15. D. Greenspan and D. Schultz, Fast finite-difference solution of biharmonic problems, *Communications of the ACM* **15** (1972).
16. J.Y. Choo, Stable high order methods for elliptic equations with large first order terms, *Computers Math. Applic.* **27** (1), 65–80 (1994).
17. M. Napolitano, Efficient ADI and spline ADI methods for the steady-state Navier-Stokes equations, *Int. J. for Numerical Methods in Fluids* **4**, 1101–1115 (1984).
18. M. Napolitano and R.W. Walters, An incremental Block-Line-Gauss-Seidel method for the Navier-Stokes equations, *AIAA Journal* **24**, 770–776 (1986).
19. R. Mei and A. Plotkin, A finite-difference scheme for the solution of the steady Navier-Stokes equations, *Computers & Fluids* **14** (3), 239–251 (1986).
20. J.D. Bozeman and C. Dalton, Numerical study of viscous flow in a cavity, *J. Comput. Physics* **12**, 348–363 (1973).
21. S.G. Rubin and P.K. Khosla, Polynomial interpolation methods for viscous flow circulations, *J. Comput. Physics* **24**, 217–244 (1977).
22. U. Ghia, K.N. Ghia and C.T. Shin, High-Re solutions for incompressible flow using the Navier-Stokes equations and a multi-grid method, *J. Comput. Physics* **48**, 387–411 (1982).